INDONESIAN JOURNAL ON GEOSCIENCE
Geological Agency
Ministry of Energy and Mineral Resources

Journal homepage: http://ijog.geologi.esdm.go.id
ISSN 2355-9314, e-ISSN 2355-9306

High Sulphidation Mineralization and Advanced Argillic Alteration within Concealed Gajah Tidur Porphyry, Grasberg District, Papua

Benny Bensaman, Mega Fatimah Rosana, and Euis Tintin Yuningsih

Faculty of Geology, Universitas Padjadjaran
Jln.Raya Bandung Sumedang KM 21, Jatinangor, Kabupaten Sumedang, Jawa Barat 45363, Indonesia

Corresponding author: bensaman@gmail.com
Manuscript received: September, 12, 2023; revised: November, 24, 2023;
approved: December, 4, 2023; available online: January, 30, 2024

Abstract - High sulphidation (HS) mineralization and associated advanced argillic alteration have been intersected by three drill holes below the Grasberg porphyry Cu-Au deposit, known as the Gajah Tidur prospect. The prospect is located between 1,500–2,750 m level, in Grasberg District, Papua, Indonesia. The holes are of KL98-10-21, KL98-10-22, and GRD39-08 which intersected 3.4 Ma Gajah Tidur monzonite, Grasberg Igneous Complex, the wall rocks of Kembelangan, and New Guinea Limestone Group. This research aims to determine the characteristics of high sulphidation mineralization associated with advanced argillic alteration at Gajah Tidur. Petrographic, XRD, SEM, fluid inclusion, and XRF (geochemical) analyses were applied to identify the mineralogy, geochemistry, and ore fluid properties. The major element plots show a differentiated intrusion. The alteration consists of potassic materials composed of biotite and K-feldspar, overprinted by phyllic and advanced argillic ones typified by alunite, pyrophyllite, and kaolinite. The high sulphidation mineralization characterized by pyrite-covellite, chalcopyrite-chalcocite, enargite, and digenite is also present. Fluid inclusion homogenization temperature of mineralized quartz vein ranges from 393 to 542°C, indicating a magmatic fluid origin predominantly. Two distinct porphyry systems, consisting of the Gajah Tidur Cu-Mo and the Main Grasberg Cu-Au porphyry systems are emplaced at the Gajah Tidur level. Advanced argillic is less intense compared to a pervasive phyllic alteration, overprinting the stockwork and surrounding rocks, emplaced at the upper part of quartz stockwork. It is possibly associated with a late stage of Gajah Tidur porphyry hydrothermal fluids which became cooler and highly acidic. Similar to other porphyry systems such as Oyu Tolgoi in Mongolia, the Gajah Tidur porphyry did not have its hydrothermal fluid ascent to the surface to form lithocap. Instead, the ascending fluids cooled at shallower depths resulting in the formation of advanced argillic alteration.

Keywords: Gajah Tidur porphyry Cu-Mo, advanced argillic, high sulphidation, alunite, enargite

How to cite this article:
Bensaman, B., Rosana, M.F., and Yuningsih, E.T., 2024. High Sulphidation Mineralization and Advanced Argillic Alteration within Concealed Gajah Tidur Porphyry, Grasberg District, Papua. *Indonesian Journal on Geoscience*, 11 (1), p.15-33. DOI: 10.17014/ ijog.11.1.15-33

Introduction

Background

Gajah Tidur is a 3.4 Ma Cu-Mo porphyry prospect (Leys *et al*., 2020). It is located adjacent and deeper than the 3.2 Ma Main Grasberg porphyry Cu-Au deposit within the Ertsberg-Grasberg mining district in Papua (Figure 1). The top of Gajah Tidur porphyry intrusion is approximately 1,500 m below Grasberg pre-mining surface, and the associated porphyry alteration and mineralization occur at elevations ranging from 1,500 to 2,750 m. Gajah Tidur exhibits a prominent phyllic alteration overprinted by barren quartz stockwork, and overlain by a substantial zone of Cu-Mo mineralization. Based on the limited

Figure 1. a). Ertsberg-Grasberg district is situated within the Central Range Fold and Thrust Belt in Papua, Indonesia. b). Projected to surface, the researched area of Gajah Tidur is depicted on the surface, falling at the southwest corner of The Grasberg open pit. the Erstberg mine pit is located at the southeast corner of the Grasberg open pit in the aerial photo (right).

drill holes intersecting the Gajah Tidur area, this study focuses on an area of high sulphidation and associated advanced argillic alteration overprinting the phyllic alteration immediately above the barren quartz stockwork.

The Ertsberg mining district encompasses several porphyry and skarn deposits (Leys *et al*., 2020), the largest of which is the Grasberg Cu-Au porphyry currently being mined by P.T. Freeport Indonesia. The Main Grasberg porphyry lies at the centre of the diatreme-hosted Grasberg Igneous Complex (GIC), which intrudes the Tertiary New Guinea Limestone Group dominated by carbonates, and the underlying Cretaceous Kembelangan and older sediments dominated by siliciclastics.

Formation of the Gajah Tidur at greater depths below the paleosurface has preserved the overlying acid-sulphate alteration and associated mineralization. In contrast, erosion has probably removed any epithermal alteration that was possibly present above the main Grasberg porphyry.

The formation of porphyry copper deposits that represent large metal anomalies raises important questions about fundamental geochemical processes on the earth crust. A detailed and rigorous understanding of their hydrodynamics and the fluid-rock reactions that drive mineral deposition requires reliable information on the pressure, temperature, and fluid composition conditions at each stage of their development.

High sulphidation mineralization and associated advanced argillic alteration overprinting phyllic alteration is an important geological phenomenon that can provide a valuable information on the mineralization potential of a deposit (Al Furqan, 2020). In the case of the Deep Grasberg deposit, particularly in the Grasberg Block Cave area, the intersection of advanced argillic alteration in two deep exploration holes is noteworthy.

Advanced argillic alteration is a type of high-temperature and more acidic hydrothermal alteration typically associated with the formation of porphyry copper deposits. It is characterized by the replacement of host-rock minerals by clay minerals such as kaolinite, dickite, and alunite. Advanced argillic alteration often occurs in the upper parts of a hydrothermal system, and is usually overprinted by other alteration types such as phyllic alteration (Hedenquist and Arribas, 2022).

Phyllic alteration is a lower temperature hydrothermal alteration associated with the development of certain types of ore deposits, including porphyry copper deposits. It is predominantly characterized by sericite (fine-grained white mica), chlorite, pyrite, and quartz. Phyllic altera-

tion occurs at shallower depths than advanced argillic alteration, and can be an important guide to mineralization.

The overprinting of advanced argillic alteration and phyllic alteration in the exploration drill holes beneath the Deep Grasberg deposit suggests the presence of a complex hydrothermal system with a potential for mineralization at depth. The intersect by drill hole of alteration zones provided valuable information in assessing the potential of the ore deposit and in planning further exploration and development programme.

This study contributes to this understanding by examining the petrography and geochemistry of the Gajah Tidur Cu-Mo porphyry system, in particular its phyllic-high sulphidation mineralization and associated advanced argillic alteration. In addition, fluid inclusions would be examined to determine the composition of hydrothermal fluids and depositional conditions, and compared with the much better studied Main Grasberg Cu-Au system and other porphyry systems worldwide. The study aims to characterize the high sulphidation mineralization and associated advanced argillic alteration hosted in the Gajah Tidur intrusion and sedimentary wall rocks within the 3,000 m to 1,500 m underground level.

Regional Geology

Papua Central Range mobile belt, which includes Ertsberg-Grasberg District is characterized by the uplift of Jurassic to Cretaceous siliciclastic sediments of The Kembelangan Group (Jkk) and carbonate formations of The New Guinea Limestone Group. This uplift is accompanied by magmatic and volcanic activity with the main product are the Grasberg Igneous Complex (GIC) and the Ertsberg Diorite (Figure 2). Fault-controlled and Late Miocene to Pliocene high-K aged of calc-alkaline to subalkaline intrusions are present throughout the Central Ranges. These intrusions are the result of partial melting of the subducted slab during collisional orogenesis, and they are thought to be associated with the final stages of the collision (Cloos *et al*., 2005).

The Grasberg porphyry, Ertsberg skarns, and other copper and gold deposits in the district are closely related to the Pliocene intrusions. The deposits were formed during the final stages of collisional orogenesis, as the result of the interaction of the intrusions with surrounding rocks and hydrothermal fluids. Grasberg porphyry Cu-Au deposit is one of the manifestations of the collision between the Australian Continent and the Pacific Plate.

The Grasberg Igneous Complex comprises three main intrusive series of ~3.11±0.05 Ma - 3.50±0.08 Ma age and extrusive units of quartz monzonitic to dioritic composition found along the Yellow Valley syncline (McMahon, 1994a). Ertsberg District itself contains at least sixteen individual intrusions, but only Dalam stage phase that has a clear evidence of contemporaneous volcanic activity. The Dalam stage formed the exterior of the GIC. The main Grasberg (Mgi) was concentrically emplaced within the Dalam rock. The Kali cuts across both the Main Grasberg and Dalam intrusions. Stockwork quartz veining is common throughout The GIC and accounts for up to 50% of the rock volume in the central part of the stockwork zone. Dalam phase is the oldest and most abundant unit within the GIC, dating to around 3.6 to 3.3 Ma. Dalam phase consist of various rock types including breccias, flow domes, and occasional tuffs and tuffaceous sediments. At higher elevations, the Dalam rocks are made up of monomict, fragmental, and magmatic breccia surrounded by a polymict, sub-volcanic breccia. At lower elevations, the Dalam rock transitions into equigranular, fine- to medium grained monzodiorite known as Dalam diorite. A number of other Pliocene rocks, mostly small intrusions occur in the Ertsberg District, but these are barren and have little associated alteration and mineralization (Leys *et al*., 2020).

Located along the southwest margin of the Grasberg Igneous Complex (GIC), a Gajah Tidur monzonite plug is distinct. This plug is characterized by a coarsely porphyritic texture, indicating that it contains relatively large crystals (phenocrysts) embedded within a finer grained ground-

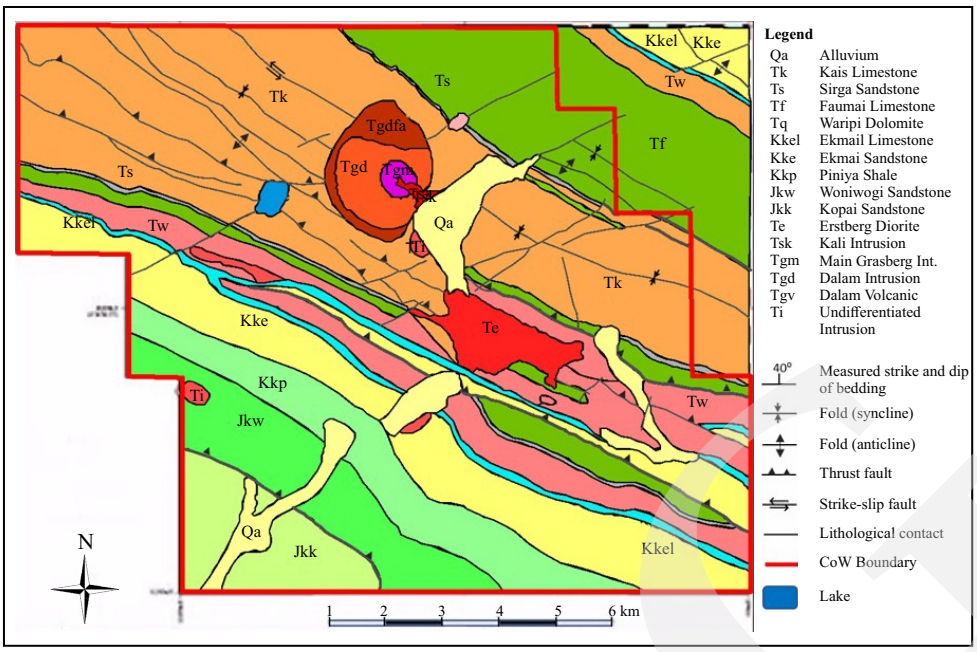

Figure 2. Ertsberg District regional geology map shows two main igneous bodies consisting of Erstberg (Te) and Grasberg Igneous Complex (GIC) intruded the Kembelangan silisiclastic sediments and New Guinea Limestone Group (modified from P.T. F.I. Ertsberg District regional geology map (2017).

mass. The groundmass of monzonite consists mainly of K-feldspar and quartz, while feldspar and biotite phenocrysts make up a significant portion of the rock composition (Figure 3).

The Gajah Tidur monzonite has a substantial vertical extent of at least 1,600 m, which provides insight into the scale and size of the intrusive body, suggesting its significance within the geological context of the area (Figure 4). The contact between the Gajah Tidur and the adjacent Dalam units is overprinted by extensive quartz veining and texturally damaging phylic alteration, making the field relationship between them unclear. However, according to zircon U-Pb dating (Trautman, 2013; Leys *et al*., 2020), the Gajah Tidur intrusion post-dates all Dalam phases, which is also corroborated by the distribution of Dalam-hosted stockwork quartz veining and related focused alteration. The Main Grasberg Cu-Au porphyry alteration and mineralization emplaced predate the Gajah Tidur Cu-Mo porphyry system.

Gajah Tidur monzonitic exhibits extensive dome-shaped quartz stockwork alteration. It

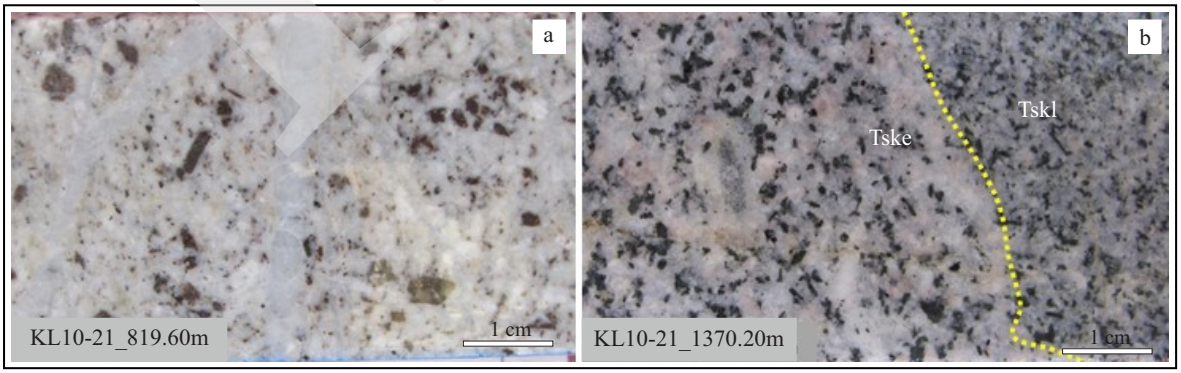

Figure 3. a). Rock slab of Gajah Tidur monzonite (Tigt), coarse hornblende altered to secondary biotite cut by quartz stockwork veins with sericite alteration selvages. b). Early Kali (Tske) monzodiorite, weakly potassic altered (2nd bio) and cut by unaltered Late Kali diorite (Tskl), KL98-10-21@819.,60 m and 1370.20m depth respectively.

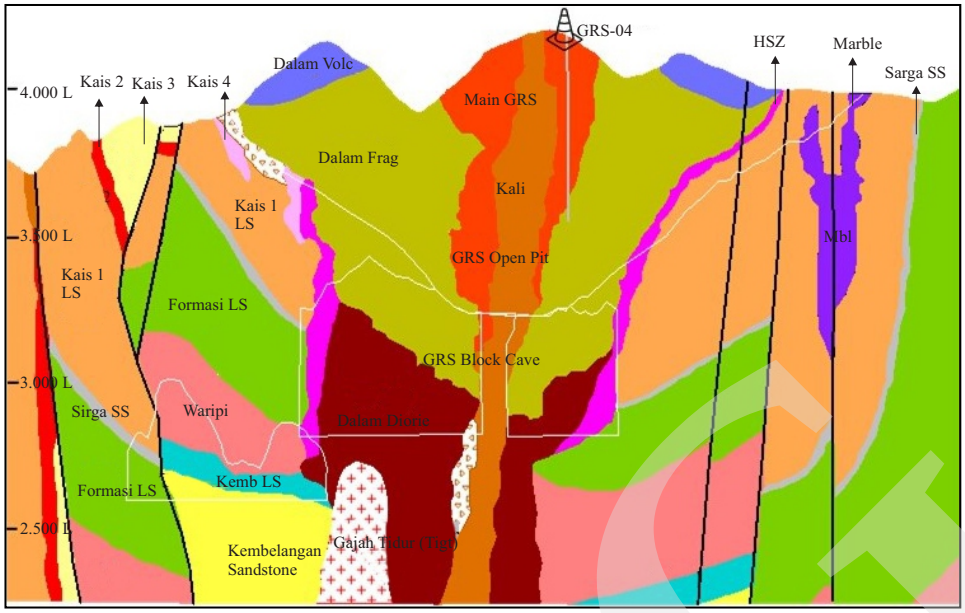

Figure 4. Looking NW Grasberg pre-mining lithology and the Gajah Tidur porphyry intrusion appearring at <3,000 m elevation, shown by yellow arrow (Leys *et al*., 2020).

extends from a depth of less than 2,400 m to an elevation of 2,800 m. The alteration is characterized by potassic rock overprinted by intense phyllic alteration which is associated with the presence of molybdenite with chalcopyrite quartz veinlets. In addition, there are pyrite-covellite veins that have overprinted the system.

In contrast, the strongly potassic altered and younger Main Grasberg (MGI) monzodiorite, extending from the surface to 2,700 m, is overprinted by a cylindrical, intense quartz-magnetite-cp-bn stockwork ~1 km in diameter. The MGI stockwork is surrounded by a 700 m wide phyllic alteration containing chalcopyrite-pyrite-covellite (Leys *et al*., 2020). Based on apatite fission-track studies (Weiland and Cloos, 1996) and recent zircon U-Pb-He studies (Wafforn, 2017), the palaeosurface at the time of GIC emplacement was less than 2 km and possibly as low as 500 m above the present surface (Mernagh *et al*., 2020).

These geological features play an important role in the distribution and formation of mineralization in the area. The geology of the region is complex and has undergone various tectonic and magmatic events over a considerable span of time. This has led to the formation of distinct geological features and mineral deposits, which are of significant interest for geological and resource exploration purposes.

Methods and Materials

Two deep exploration holes, KL98-10-21 and KL98-10-22, were drilled from subsurface at 3,020 m level. The holes were logged, sampled, and subjected to petrographic analysis. In addition, XRD (X-Ray Diffraction), XRF (X-Ray Fluorescence), SEM-EDS (Scanning Electron Microscopy-Energy Dispersive X-Ray Spectroscopy), and freezing-heating stage fluid inclusion techniques were used. The holes reached an elevation of 1,500 m and represent the deepest level drilled in the district to date.

This study consisted of drill core logging from three drill holes consisting of KL98-10-21, KL98-10-22, and GRD39-08, which conducted to examining and recording details about the core obtained from drilling. It includes observations about the rock type, any changes in lithology, signs of alteration, presence of mineralization, and other geological features.

Selected half of the drill core samples were washed and photographed, providing a visual

record of the samples. The scale and depth of the drill hole were included in the photographs for reference. Thinner cut of the half drill core is also prepared like a slab for petrology purpose, then to describe the rock mineralogy using a loupe and a microscope.

A total of ninety-seven drill core samples were collected showing the black dots in the drill section at Figure 5. Selected unaltered and altered core slabs were then made into thin sections, polished sections and doubly polished section for petrographic, ore microscopic, SEM, and fluid inclusion analyses, respectively. The samples were also prepared for XRF and XRD analyses.

Samples taken from the drill core were subjected to various analytical techniques at the Department of Earth Resource Engineering Laboratory, Kyushu University, in Fukuoka, Japan, to identify the host rock lithology, alteration mineralogy and geochemistry, as well as mineralization of the researched drill holes at Gajah Tidur level area.

Sample characterization included petrographic examination, XRF, XRD, SEM-EDS, and fluid inclusion analyses. These techniques were used to determine the nature of the protolith, to identify alteration mineralogy, paragenesis (sequence of mineral formation) and patterns. Major and trace element geochemistry were also analyzed.

XRD was used to identify clay and other fine-grained hydrous alteration minerals. The presence of sulphide mineralization was investigated using reflected light microscopy and SEM-EDS (energy dispersive X-ray spectroscopy). Fluid inclusions were also examined to understand the composition of the hydrothermal fluids responsible for ore formation and to determine the pressure-temperature (P-T) conditions under which the minerals were deposited.

Overall, this comprehensive approach combining various analytical techniques aims to provide a thorough understanding of the alteration mineralogy and characteristics of the core samples, and to elucidate the processes involved in the formation of the altered and mineralized Gajah Tidur intrusion and its sedimentary wall rocks.

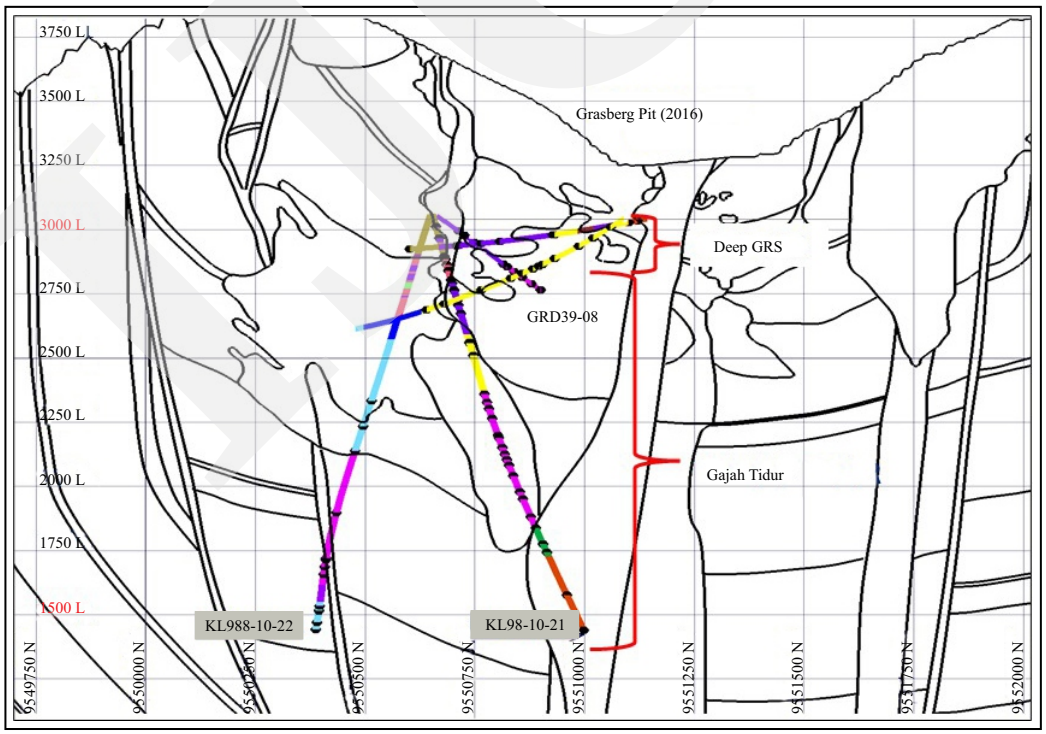

Figure 5. Sample location on NW−SE drill cross section (black dots) in three drill holes (KL98-10-21, KL98-10-22, and GRD39-08).

Result and Analysis

Subsurface Geology

The geology of Ertsberg District is complex which has undergone various tectonic and magmatic events over a considerable span of time. The complexity of the geology including structure and lithology have led to the formation of distinct geological features and mineral deposits, which are of significant interest for geological and resource exploration purposes.

Local geology at Gajah Tidur area is interpreted based on drill core mapping, supported by petrographic and XRF analyses. The petrographic analysis has been applied for relatively fresh rock samples, while the XRF analysis of trace elements result was used to determine the rock types for altered samples. Drill core logging conducted on three drill holes consisted of KL 98-10-21, KL98-10-22, and GRD39-08. The aim is to characterize the lithology, alteration, and mineralization, and resulted in a drill-hole geology cross-section of Gajah Tidur intrusion.

Subsurface geology in between 2,750 m to 1,500 m level of Gajah Tidur area comprises quartz sandstone, limestone, and shale of Ekmai Formation, overlying Waripi dolomitic limestone and Faumai fossiliferous limestone of New Guinea Limestone Group. Those sediment and carbonate sequences have been intruded by monzonitic to dioritic rock of Dalam Unit, Main Grasberg, and Kali of Grasberg Igneous Complex (GIC), and then Gajah Tidur monzonite and undifferentiated feldspar porphyry (Figure 6).

Strongly altered and mineralized Dalam diorite overlies the Gajah Tidur intrusion, which have been studied petrographically to highlight the differences in their primary mineralogy, alteration, mineralization, and textures. The key features and core slab description of Dalam diorite and Gajah Tidur monzodiorite and thin section petrographic description are described in Figure 7. The summary of drill core logging has also been described in Tables 1 - 3.

Whole-rock Geochemistry

A total of ten drill core samples were selected for XRF analysis, comprising less altered rocks that were prepared as press pellets. This method is crucial for quantifying the geochemical composition using Rigaku XRF spectroscopy. The preparation and analysis of samples for major oxide and trace element analyses were conducted at the Department of Earth Science Laboratory, Kyushu University, in Fukuoka, Japan.

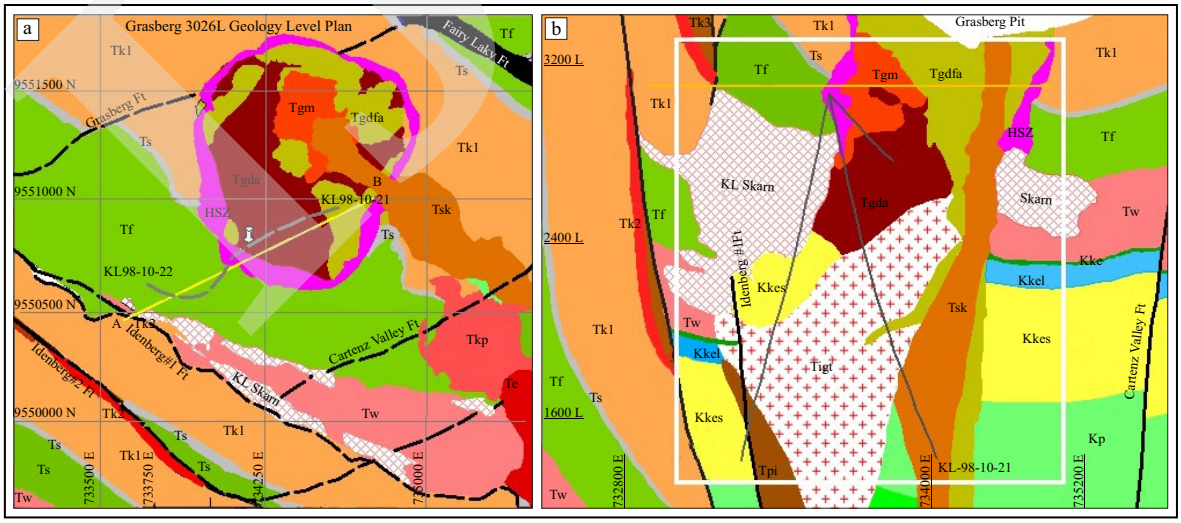

Figure 6. a). Gajah Tidur geology map at 3,026 mL and KL98-10-21 and KL98-10-22 and b). Geology cross section, consisting of Kembelangan silisiclastic (Kp, Kkes, Kkel, Kkeh) and New Guinea Limestone Group (Tw, Tf, Ts, Tk) intruded by Grasberg Igneous Complex (GIC) consisting of Tgd, Tigt (Gajah Tidur), Tgm and Tsk (modified internal P.T. Freeport Indonesia, 2017).

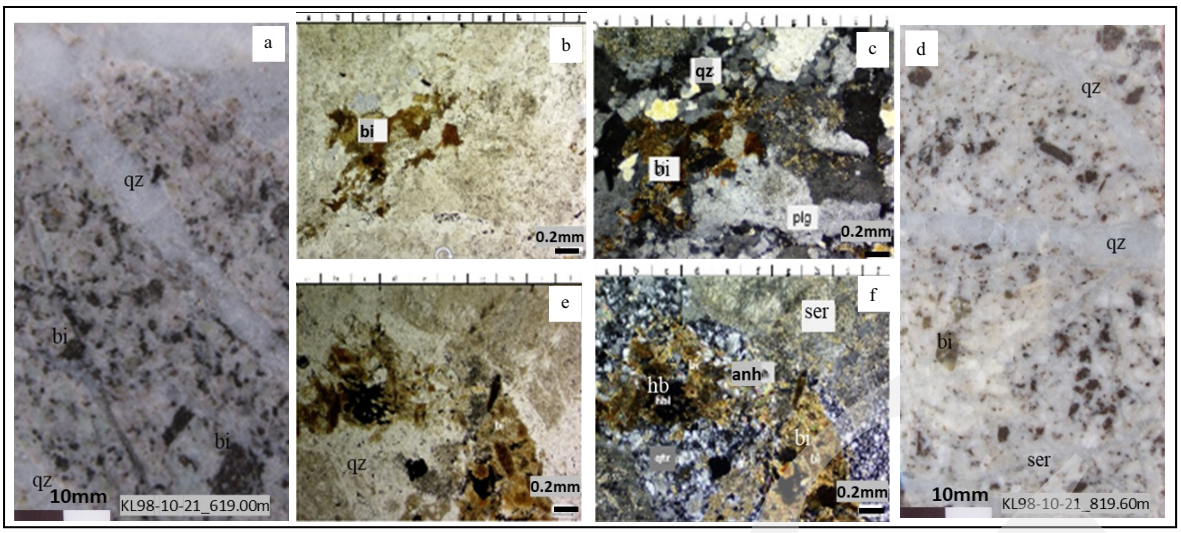

Figure. 7. (a) Potassic altered Dalam diorite composed of 2nd biotite-K-feldspar and quartz-K-feldspar groundmass cut by qz veins, porp.texture, hb altered to secondary biotite. (b) Dalam diorite transmitted light photomicrograph; brown bio in qz-ser-anh groundmass; (c) Reflected light photomicrograph showing opaque minerals; (d) Gajah Tidur monzodiorite, qz-ser-br-bi alteration;(e) Gajah Tidur transmitted light photomicrograph showing qz-ser-br-biotite; and (f) Gajah Tidur reflected light photomicrograph showing some opaque minerals.

Table 1. KL98-10-21 Summary Logging

Depth (m)	Lithology	Alteration	Mineralization	Sample (Depth)
0 – 271	Faumai and Waripi Fms; limestones; qz ss, dolomimite	Rs, mbl, hf, sk, qz-py and secondary bi dikes	Anh-py-cp-cv, locally massive form and veinlets	51.75m; 97.7; 169.6; 181; 182.3; 203.6; 227.8; 264.7
271 - 716	Dalam andesite and diorite	Qz-ser-py overprint 2nd bi-Kf	Qz-py-cv-cp disseminated and veinlets	277.4; 304.3; 307.2; 348; 365.4; 398.9; 513.9;516.7; 566.3
716 - 1,266	Gajah Tidur monzodiorite	Stk qz-ser-py overprint secondary bi-Kf	Qz-py-cv-cp±bn-mo disseminated and veinlets	720.5; 754.3; 779.3;819.6; 886.7; 897.6; 936.8; 963.25; 985.2; 1008.95; 1009.3; 1052.5; 1118.95; 1147.3
1,266-1,700 (EOH)	Early and Late Kali monzodiorite	Chl-ep and minor 2nd bi after mafic	minor qz-Kf-py±cp veinlets	1268.2; 1334.7; 1370.2;1550; 1699.5

Table 2. KL98-10-22 Summary Logging

Depth (m)	Lithology	Alteration	Mineralization	Sample (Depth)
0 - 421	Faumai and Waripi Fms. limestones, qz ss, dolomite	Mbl, hf, rs, sk, sil-py and 2nd bi-Kf	Massive mt-py-cv-cp and veinlets	25.1; 217.2; 236.3; 262.1
421 - 952	Ekmai shale, limestone and ss	Hf, sk, qz-py	Qz-py-cp	699.35; 706.8; 749.3; 852.5
952 - 1504	Gajah Tidur monzodiorite	2nd bi-Kf overprint by qz-ser-aa-py-cv	Qz stk-py-bn-cv-cp-mo disseminated and veinlets	952.4; 1203.8; 1392; 1398.3 ;1429.1; 1460.2
1504 - 1578	Tertiary Pliocene diorite	Qz-ser; chl-epi-py	Minor py disseminated and veinlets	N/A
1578 – 1700 (EOH)	Ekmai Sandstone	Qz-weak sk	Qz-anh-py disseminated and veinlets	1595.5; 1616.2; 1667.5; 1698.6

Table 3. GRD39-08 Summary Logging

Depth (m)	Lithology	Alteration	Mineralization	Sample (Depth)
0 – 93.7	HSZ (High Sulphide Zone)	Replacement py-mg-hm (HSZ) and minor qz-ser-py	Minor disseminated cp-bn-cv	N/A
93.7 – 296.6 (EOH)	Dalam andesite (Tgda)	Qz-ser-py overprints secondary bi	Disseminated and vein-hosted py-cv-cp ± mo	101.3; 123.4; 162.3; 283.7
296.6 – 434.1	Dalam diorite (Tgdd),	qz-ser-py overprint secondary bi-Kf, qz stk veins	Py-cv-cp disseminated and veinlets	299; 326.2; 358.45; 395.7; 431.8

The mobility of major oxides, such as SiO_2, K_2O, Na_2O, and MgO is contingent upon the intensity and type of hydrothermal alteration. Consequently, only the samples from fresh and mildly altered intrusions were collected for analysis, and were employed in the intrusion classification based on major oxides. A plot of total alkali ($K_2O + Na_2O$) *vs.* SiO_2, utilizing Cox *et al.* (1979) Total Alkali Silica (TAS) classification, was performed. The oxide normalization was carried out, rendering the total major oxide in a sample an intact volume without considering the volume of "Loss on Ignition" (LOI). The average LOI for the Gajah Tidur intrusion is 2.0 wt. %, compared to 1.8 wt. % for the Dalam diorite, 4.2 wt. % for the Ertsberg intrusion, and 3.2 wt. % for the Karume intrusion. Tertiary Pliocene intrusive (Tpi), and Kali monzodiorite have the average of 4.67 wt. % and 1.35 wt. %, respectively (Table 4 and Figure 8).

Based on the TAS plot diagram using total alkali data, the Gajah Tidur intrusion (Tigt) is categorized as an alkali granite type, similar in composition to the Dalam diorite (Tgdd) and the Late Kali monzodiorite (Tskl) of the Grasberg Igneous Complex (GIC). Gajah Tidur intrusion is identified as a monzodiorite that does not extend to the surface of the Grasberg intrusion as GIC does. Additionally, the XRF data plot diagram of subalkalic rock subdivision, utilizing the K_2O vs. SiO_2 ratio, indicates that the Grasberg Igneous Complex mostly falls within a high-K (calc-alkaline) series of intrusive rocks, includ-

Table 4. XRF Analysis Result of Major Elements

No	Sample ID	Lith	SiO_2	TiO_2	Al_2O_3	FeO	MnO	MgO	CaO	Na_2O	K_2O	P_2O_5	LoI
1	KL98-10-21_720.50	Tgdd	71.014	0.298	13.059	1.254	0.001	1.568	0.422	0.473	9.251	0.022	1.86
2	KL98-10-21_886	Tgdd	80.107	0.158	7.186	1.76	0	0.694	0.673	0.413	4.139	0.025	2.73
3	KL98-10-21_1118	Tgdd	77.822	0.264	9.448	1.186	0.002	1.368	0.711	0.891	6.428	0.046	1.13
4	KL98-10-21_1221	Tgdd	70.876	0.354	11.776	1.59	0.022	1.585	1.625	1.28	7.509	0.282	2.15
5	KL98-10-21_1550	Tske	63.567	0.427	15.499	4.613	0.059	1.745	4.54	2.965	3.416	0.282	1.34
6	KL98-10-22_1595	Tpi	57.653	0.53	14.229	5.342	0.075	2.763	6.048	2.208	3.551	0.362	4.67
7	KL98-10-21_1699	Tske	63.165	0.508	15.573	4.425	0.081	1.958	5.309	2.81	3.616	0.302	1.43
8	KL98-10-22_217.20	Tgda	57.518	0.415	13.538	1.439	0.163	2.387	6.869	0.454	9.947	0.296	6.13
9	KL98-10-22_1595	Tpi	57.653	0.53	14.229	5.342	0.075	2.763	6.048	2.208	3.551	0.362	4.67
10	KL98-10-22_1616	Tpi	56.901	0.529	14.419	5.436	0.117	2.949	6.26	2.236	3.463	0.363	5.38
11	KL98-10-22_1667	Kkes	64.468	0.525	2.282	11.632	0.254	0.836	13.384	0.376	0.189	0.329	2.65
12	GRD39-08_162.3	Tgda	66.892	0.239	17.82	2.013	0	0.983	0.131	0.339	4.837	0.096	4.1
13	GRD39-08_299	Tigt	62.663	0.379	16.165	2.266	0.012	2.044	0.344	0.397	10.298	0.222	3.17
14	GRD39-08_326.20	Tigt	69.276	0.279	14.138	1.843	0	0.966	0.097	0.366	8.321	0.083	2.4
15	GRD39-08_358.45	Tskl	68.787	0.289	13.493	1.65	0.008	1.682	0.278	0.502	9.747	0.013	1.73
16	GRD39-08_431.8	Tigt	64.109	0.36	16.275	2.194	0.024	1.615	0.595	0.49	9.388	0.026	3.18

ing The Early Kali (Tske) and Late Kali (Tskl) intrusions (Figure 8).

Hydrothermal Alteration

The siliciclastic sedimentary wall rocks of the holes KL98-10-21 and KL98-10-22 were intruded by medium-grained Dalam hornblende trachy andesite (Tgda) at a depth of 263 m. This intrusion was followed by Dalam diorite (Tgdd), Kali monzonite (Tsk), and finally the Gajah Tidur intrusion (Tigt). The intrusive rocks have undergone both phyllic and advanced argillic alterations, which are characterized by quartz-sericite-covellite-pyrite assemblages and advanced argillic alteration assemblages composed of pyrophyllite-kaolinite-alunite. In some areas, alteration patches of epidote-phlogopite-chlorite-garnet-pyrite endoskarn were observed, which are then cross-cut by quartz-anhydrite-pyrite veins.

MacDonald and Arnold (1994) indicated that kaolinite was commonly linked with sericite at the upper part of the Grasberg system, extending down to a depth below 3,400 m, with the kaolinite content decreased with the increasing depth. Quantitative XRD analysis of pulp samples collected from the phyllic alteration zone identified advanced argillic mineral assemblages consisting of less than 2% pyrophyllite and alunite. Furthermore, this analysis revealed the presence of zunyite, diaspore, dickite, and svanbergite (Allen, 2012).

Although the advance argillic alteration is not as pronounced, a high sulfidation mineralization comprising covellite-pyrite±enargite is commonly encountered in the phyllic alteration zone adjacent to the Gajah Tidur stockwork zone. Phyllic and advanced argillic alterations at Gajah Tidur, composed of sericite-kaolinite-anhydrite-pyrite, are possibly introduced during the late stages of the Grasberg hydrothermal system (Figure 9).

A breccia texture is present on the south side of the Early Kali at the 2,800 m level, indicating a hydrothermal system with the presence of a breccia zone. This zone comprises unmineralized Early Kali and quartz-veined and mineralized Dalam rock fragments. It contains over 4% kaolinite, associated with anhydrite-pyrite-covellite, and is intersected by native sulfur, representing a feature of the late phase of the Grasberg hydrothermal system.

Hole GRD39-08 collared on replacement sulphide alteration (HSZ), characterized by chlorite-epidote-garnet alteration containing more than 20% pyrite-pyrrhotite, magnetite-hematite, and chalcopyrite. These minerals were hosted by both intrusive and wall rock. The hole then encountered Dalam andesite at a depth of 94 m, where intense quartz-sericite-pyrite-covellite alteration indicative of phyllic and advanced argillic alteration was observed.

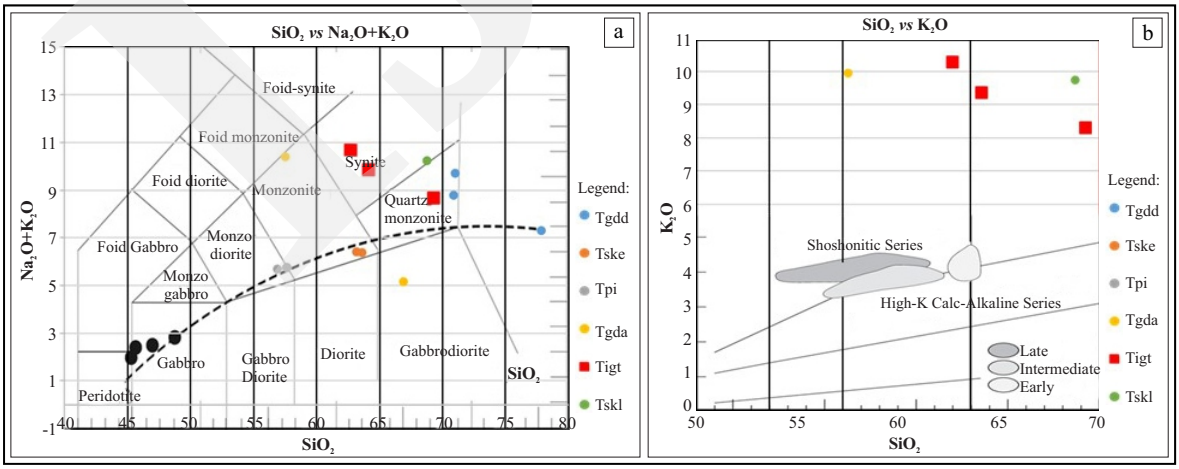

Figure 8. (a) Gajah Tidur monzodiorite (red square) XRF plot reveals its classification as quartz monzonite and syenite, similar to The Dalam diorite (Tgdd) and Kali monzodiorite (Tskl). The intrusive exhibits a high silica content, potentially linked to silica flooding and veining. (b) K_2O vs. SiO_2 ratio diagram from the XRF data plot shows that Gajah Tidur and Kali (Tsk) intrusions are categorized to shoshonitic series.

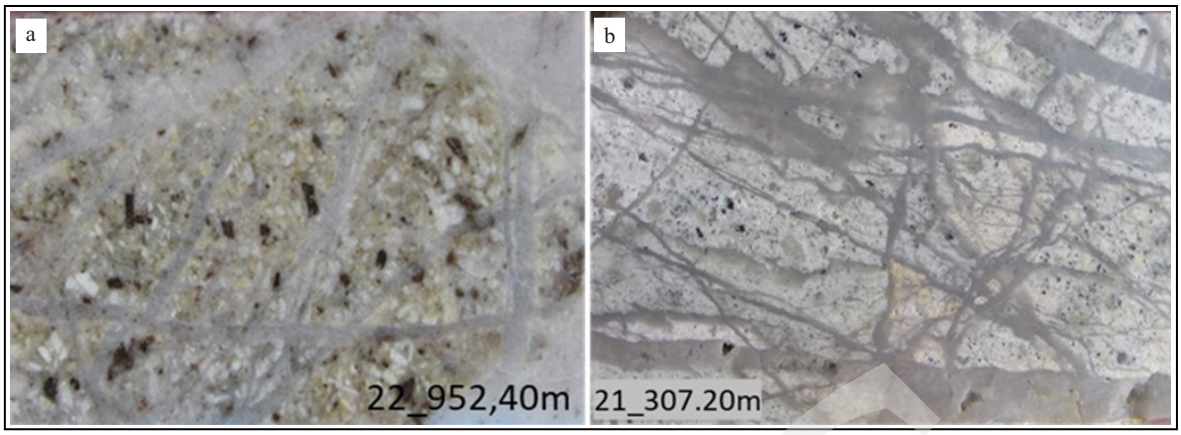

Figure 9. a). Phyllic altered Gajah Tidur monzonite with earlier brown secondary biotite and white mottled of clay alteration of pyrophyllite-alunite and b). intense silica-sericite alteration cross cutting barren quartz veinlets.

At a greater depth within the hole, Dalam diorite was encountered to have undergone phyllic and advanced argillic alteration, featuring quartz-sericite-pyrite alteration, as well as pyrophyllite-alunite-kaolinite-anhydrite alteration. The distribution and geometry of the phyllic and advanced argillic alteration zones were interpreted based on the megascopic description provided by the drill core. This interpretation was further supported by quantitative XRD and NIR analyses, which were plotted on the Gajah Tidur alteration plan view at the level of 2,600 m and alteration cross-section, as illustrated in Figure 10.

Quantitative X-ray Diffraction (XRD) analysis calibrated Inductively Coupled Plasma (ICP) geochemistry has identified alunite (Figure 11), pyrophyllite (Figure 12), also kaolinite and dickite along with high sulphidation mineralization including minor enargite as seen in Figure 13 and Table 5. The presence of these minerals indicates the occurrence of specific alteration processes and conditions in the geological setting. Additionally, the presence of high sulphidation mineralization, including minor enargite, suggests the presence of sulfide minerals in the area, which can have economic implications in terms of mineral resources.

Vein/Veinlet System and Ore Mineral Paragenesis

Hydrothermal alteration paragenesis in the researched area was initiated by potassic alteration with the formation of secondary brown biotite in

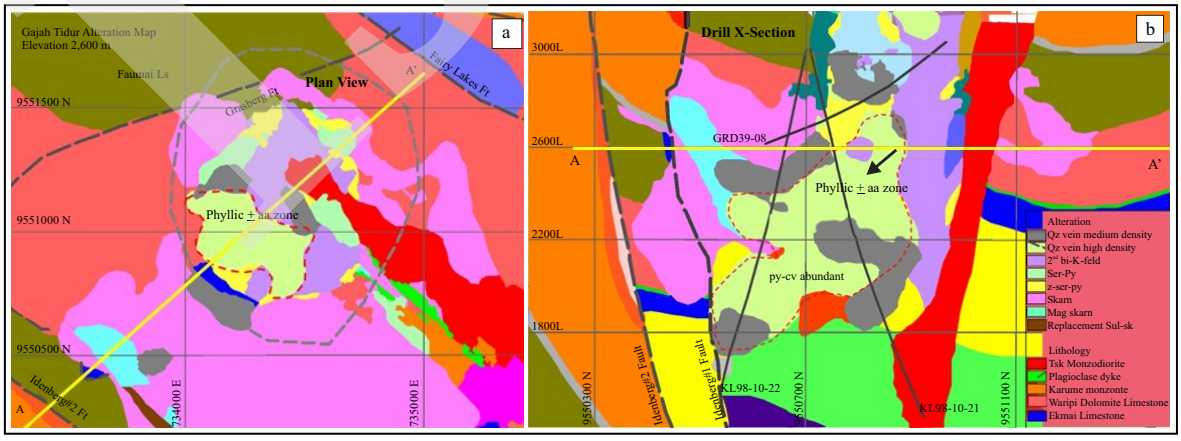

Figure 10. a). Gajah Tidur alteration map 2,600 m level, intense quartz stockwork vein zone (pale green) associated with quartz-sericite-pyrite-covelite and pyrophylite-kaolinite-alunite alteration zone based on drill core mapping, NIR and quantitative XRD analysis. b). X-section facing NW, showing KL98-10-21, KL98-10-22, and GRD29-08 drill holes and alteration zonation based on drill core logging (modified from P.T. F.I. alteration model, 2012).

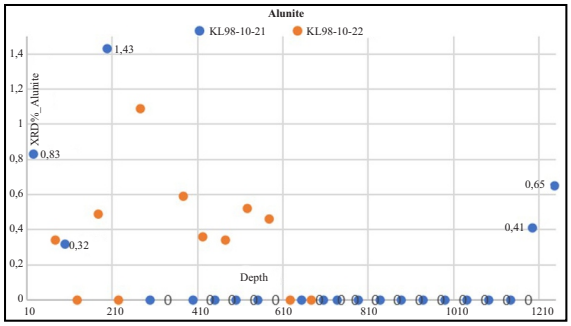

Figure 11. Quantitative XRD analysis result of alunite at hole KL98-10-21 KL98-10-22 which has the average concentration of 0.4 – 3.5 % wt and the highest content is at KL98-10-21, arround 200 m depth.

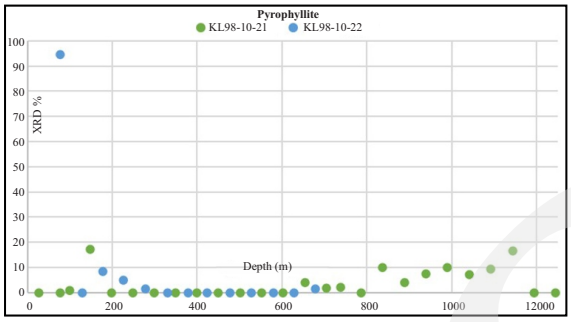

Figure 12. Quatitative XRD analysis result of pyrophylite shows more presence at KL98-10-21 @ >800 – 1,100 m depth and KL98-10-22 has the content of less pyrophylite.

the Gajah Tidur intrusion, overprinted by phyllic and advanced argillic alteration. Phyllic alteration is characterized by less mineralized to barren silica flooding and cross cutting recrystallized quartz veins. The alteration has also affected the surrounding Ekmai sandstone, leading to the formation of greyish-white quartz stockwork zones. The advanced argillic associated with high sulphidation mineralization are often of interest in mineral exploration, as they can be associated with the deposition of valuable minerals like gold, copper, or other economically important substances.

SEM-EDS analysis of potassic altered Dalam diorite sample at GRD39-08_114.10 m has showed the presence of Cu-As and Sb elements that includes enargite which commonly associated with high sulfidation mineralization. SEM-EDS analyses have also identified other copper sulphide mineral such as chalcopyrite, bornite, covellite, locally chalcocite, and diginite (Figure 14).

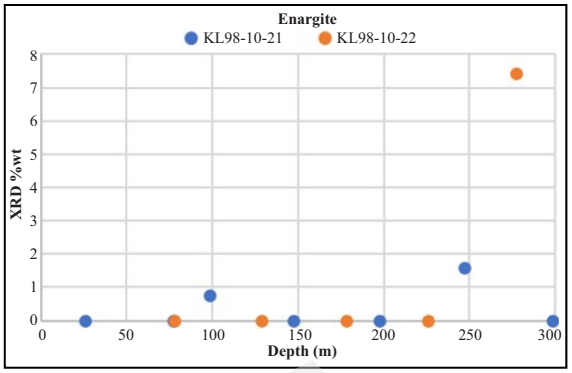

Figure 13. Quantitative XRD analysis result of enargite occurs up to >7 % wt at KL98-10-22 around 275 m depth.

The identification of Cu, As, and Sb along with the presence of enargite and quartz veining, is consistent with the characteristics of a high sulfidation mineral assemblage. High sulfidation systems typically involve the deposition of minerals through hydrothermal fluids rich in sulfur, which can result in the formation of copper, arsenic, and antimony-bearing minerals.

Drill core logging and microscopic study have concluded that the mineralization paragenesis at Gajah Tidur is divided into four types (Figure 14) : (1) quartz-secondary biotite veinlets which probably predate the quartz stockwork vein, (2) disseminated pyrite-covellite-chalcopyrite in potassic-phyllic altered Gajah Tidur porphyry and hornfelsic sandstone, (3) potassic altered (2nd biotite) porphyry around brecciated quartz veins, (4) chalcopyrite±molybdenite-anhydrite veinlets cutting the quartz stockwork of Gajah Tidur porphyry. In the Early Kali monzodiorite, chalcopyrite is accompanied by anhydrite without quartz, since the intrusion has no quartz vein. The presence of chalcopyrite and anhydrite indicates the potential for porphyry copper alteration and mineralization.

Gajah Tidur prospect alteration and mineralization mineralogy were also identified through mineragraphic analysis as shown by Figure 15. The prospect has indicated a complex geological setting with multiple types of mineralization associated with various alterations and geological features. These findings are valuable for understanding the mineral potential of the Gajah Tidur area, and may

Table 5. XRD Analysis Result

Hole ID	Depth	Lith	Alu	Anda	Apa	Bor	Cp	Cov	Dic	Enar	Mag	Mal
KL98-10-21	25	Tf	0.83	21.7	Tf	0	0	3.68	0	0	0	0
KL98-10-21	76	Tf	0	0	0	0	0	0	0.27	0	0	0
KL98-10-21	97	Tgda	0.32	1.04	0.17	0	0	5.88	0	0.76	13.91	0
KL98-10-21	145	Tf	3.2	36.83	Tf	0	0	17.73	2.69	0	0	0
KL98-10-21	196	Tw	1.43	5.19	3.02	0	4.71	20.3	5.53	0	23.04	0
KL98-10-21	246	Tw	3.44	2.48	5.5	0	7.34	9.79	16.74	1.58	25.37	0
KL98-10-21	347	Tgda	2.44	0	0	0	0	0	0	0	0	0
KL98-10-21	499	Tgdd	0	0	0	0	0	0	0	0	3.57	0
KL98-10-21	550	Tgdd	1.98	0	0	0	0	0	0	0	0	0
KL98-10-21	601	Tgdd	3.1	0	0	2.53	0	0	0	0	0	0.85
KL98-10-21	651	Tgdd	0	0	0	0	0	0	0	0	0	16.77
KL98-10-21	702	Tgdd	0	0	0	0	1.46	0	0	0	0	0
KL98-10-21	736	Tigt	0	0	0	0	1.3	0	0	0	0	4.11
KL98-10-21	784	Tigt	0	0	0	0	1.55	0	0	0	0	23.62
KL98-10-21	835	Tigt	0	0	0	0	1.28	0	0	0	0	34.15
KL98-10-21	886	Tigt	0	0	0	0	2.09	0	0	0	0	38.51
KL98-10-21	937	Tigt	0	0	0	0	1.47	0	0	0	0	40.42
KL98-10-21	988	Tigt	0	0	0	1.33	0	0	0	0	0	45.25
KL98-10-21	1039	Tigt	0	0	0	0	0	0	0	0	0	26.14
KL98-10-21	1090	Tigt	0	0	0	0	0	0	0	0	0	35.39
KL98-10-21	1141	Tigt	0	0	0	0	0	0	0	0	0	42.75
KL98-10-21	1192	Tigt	0.41	0.68	0	0	4.8	0	0	0	0	0
KL98-10-21	1243	Tigt	0.65	0	0	6.07	0.74	0.98	0	0	0	0
KL98-10-21	1297	Tskl	1.69	0	0	2.57	0	0	0	0	0	0
KL98-10-21	1348	Tskl	1.67	0	0	3.98	0	1.69	0	0	0	0
KL98-10-21	1399	Tske	1.85	0	0	3.47	0	0	0	0	0	0
KL98-10-21	1450	Tske	1.99	0	0	1.92	0	0	0	1.42	0	0
KL98-10-22	76.5	Tf	0.34	1.37	0	0	0	94.6	0.8	0	0	0
KL98-10-22	127.5	Tf	0	0	0	96.4	0	0	0	0	0	0
KL98-10-22	177	Tw	0.49	5.3	0	0	0	65.09	0	0	0	0
KL98-10-22	224	Tgda	0	0	2.36	9.2	1.61	0	0	0	0	10.81
KL98-10-22	276	Tw	1.09	2.56	18.16	0		2.39	4.33	7.42	3.24	32.43
KL98-10-22	328	Tw	1.63	3	12.32	0	7.89	4.17	13.07	0	9	0
KL98-10-22	377	Tw	0.59	2.31	2.06	0	0	1.46	47.97	0	1.15	0
KL98-10-22	422	Kkeh	0.36	0.93	0	1.4	2.43	9.61	0.93	0	8.64	0
KL98-10-22	476	Kkel	0.34	0	0	0	1.17	15.89	0	0	0	0
KL98-10-22	536	Kkes	0.52	0	0	5.39	0	1.79	0	0	0	0
KL98-10-22	578	Kkes	0.46	0	0	0	0	1.82	0	0	0	0
KL98-10-22	626	Kkes	0	0	0	0	1.42	0	1.21	0	0	7
KL98-10-22	677	Kkes	0	0	0	0	1.02	0	0	0	0	0
GRD39-08	101	Tgda	0	0	0	0	0.55	1.25	0	0	0	0
GRD39-08	149	Tgda	0	0	0	0	0.43	0.93	0	0	0	0
GRD39-08	200	Tgda	0	0	0	0	1.6	0	0	0	0	0
GRD39-08	251	Tgda	0	0	0	0	0.86	0	0	0	0	0
GRD39-08	301	Tigt	0	0	0	0	2.38	0	0	0	1.01	0
GRD39-08	351	Tigt	0	0	0	0	1.9	0	0	0	0	0

Table 5. continued...

Hole ID	Depth	Lith	Moly	Peri	Pyro	Pyrop	Sph	Spin	Sul	Talc	Top	Zeo	Zuny
KL98-10-21	25	Tf	0	0	3.55	0	0	0	0	0	0	3.8	0
KL98-10-21	76	Tf	3.49	0	0	0	0	0	0	1.6	3.6	0	0
KL98-10-21	97	Tgda	0	0	27.29	0.97	0	0	2.89	0	31.35	11.56	2.7
KL98-10-21	145	Tf	0	0	0	17.14	0	0	2.93	3.35	0	2.1	0
KL98-10-21	196	Tw	0	0	0	0	0	0	0	12.96	3.89	8.86	4.3
KL98-10-21	246	Tw	0	0	0	0	0	0	0	6.1	0.95	8.43	9.8
KL98-10-21	347	Tgda	0	0	0	0	0	0	0	93.5	0.3	0	0
KL98-10-21	499	Tgda	0	0	0	0	0	1.77	0	0	86.82	0	0
KL98-10-21	550	Tgda	0	0	0	0	0	0	0	96.28	0.3	0	0
KL98-10-21	601	Tgda	0	0	0	0	0	0	0	97.32	0.3	0	0
KL98-10-21	651	Tgdd	1.37	0	0	0	0	0	0	80.74	1.6	0	0
KL98-10-21	702	Tgdd	0.91	0	0	0	0	0	5.02	0	88.73	0	0
KL98-10-21	736	Tgdd	0	0	0	0	2.2	0	0	0	87.22	0	0
KL98-10-21	784	Tgdd	0	0	0	4.06	0	5.59	0	70.88	0.7	0	0
KL98-10-21	835	Tgdd	0	0	0	1.76	0	13.54	0	78.12	1.6	0	0
KL98-10-21	886	Tigt	0	0	0	1.97	0	7.46	0	82.82	1.1	0	0
KL98-10-21	937	Tigt	0	0	0	0	0	5.76	0	65.79	1.4	0	0
KL98-10-21	988	Tigt	0	0	0	9.99	0	0	0	48.24	1.6	0	0
KL98-10-21	1039	Tigt	0	0	0	3.89	0	10.52	0	38.66	1.8	0	0
KL98-10-21	1090	Tigt	0	0	0	7.43	0	4.19	0	40.45	1.8	0	0
KL98-10-21	1141	Tigt	0	1.33	0	9.88	0	2.82	0	35.14	1.6	0	0
KL98-10-21	1192	Tigt	0	0	0	7.04	0	4.93	0	58.79	1.2	0	0
KL98-10-21	1243	Tigt	0	0	0	9.19	0	0.89	0	47.93	1.3	0	0
KL98-10-21	1297	Tigt	0	0	0	16.73	0	1.98	0	31.56	1.3	0	0
KL98-10-21	1348	Tigt	0	42.23	0	0	0	19.01	0	0	0	1.5	0
KL98-10-21	1399	Tigt	33.67	0	0	0	26.83	0	0	0	29.07	0	0
KL98-10-21	1450	Tskl	18.84	0.69	0	0	51.97	0	1.66	0	17.39	0	0
KL98-10-21	76.5	Tskl	16.37	0	0	1.16	51.87	0	1.44	0	15.79	0	0
KL98-10-21	127.5	Tske	18.59	0	0	1.06	51.63	0	1.63	0	15.92	0	0
KL98-10-21	177	Tske	19.45	0	0	0	50	0	4.31	0	15.85	0	0
KL98-10-22	224	Tf	0	0	0	94.6	0	0	0	0	0	0	0
KL98-10-22	276	Tf	0	96.4	0	0	0	0	0	0.87	0	0	0
KL98-10-22	328	Tw	0	0	0	8.48	0	0	0	0	0	5.7	0
KL98-10-22	377	Tgda	0	8.35	0	5.05	0	20.68	0	25.4	2.9	0	0
KL98-10-22	422	Tw	0	0	2.82	1.38	0	0.97	0	5.44	7.89	0	1.61
KL98-10-22	476	Tw	0	9.87	0	0	0	0	7.15	3.51	0	1.71	4.4
KL98-10-22	536	Tw	0	12.57	0	0	0	1.58	0.69	2.42	1.61	0	3.3
KL98-10-22	578	Kkeh	5.8	23.8	0	0	0	11.88	4.14	9.71	0	10.6	0
KL98-10-22	626	Kkel	28.95	0	0	0	26.87	15.55	0	0	5.63	0	0
KL98-10-22	677	Kkes	24.73	0	0	0	4.09	0	0	0	62.32	0	0
KL98-10-22	101	Kkes	4.33	0	0	0	3.19	2.13	5.11	0	81.17	0	0
KL98-10-22	149	Kkes	0	0	0	0	0	6.73	0	80.99	0.9	0	0
KL98-10-22	200	Kkes	0	0	0	1.63	1.7	3.78	0	90.35	0.1	0	0
GRD39-08	251	Tgda	0	0	0	0	0	0	0	3.41	0	0	0
GRD39-08	301	Tgda	0.14	0	0	0	0	0	0	5.14	0	0	0
GRD39-08	351	Tgda	0	0	0	0	0	0	0	3.87	0	0	0

Alu: Alunite Apat: Apatite Cp: Chalcopyrite Dic: Dickite Mag: Magnetite Anda: Andalusit Bor: Bornite Cov: Covellite
Dic: Dickite Mal: Malachite Mol : Molybdenite Pyro: Pyrolusite Sph: Sphalerite Sul: Sulfur
Topaz: Topasz Sph: Sphalerite Sul: Sulfur Peri= Priclase Pyrop: Pyrophylite
Spin: Spinel Talc: Talc Zeo: Zeolite Spin: Spinel Zuny: Zunyite

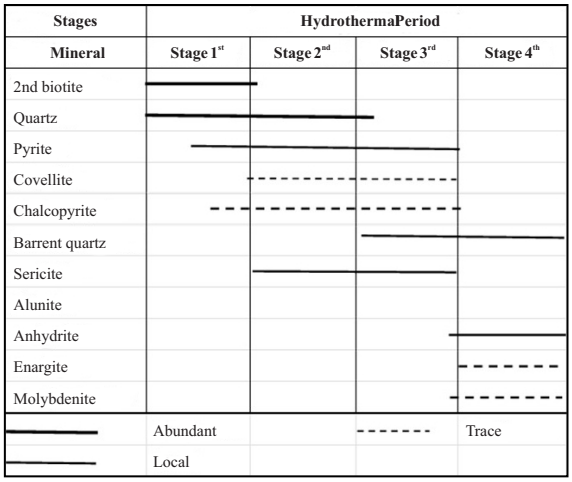

Figure 14. Alteration-mineralization paragenesis of Gajah Tidur area.

be of interest in mineral exploration and resource assessment. Further geological and geochemical studies would likely be conducted to assess the economic viability of these mineral deposits.

Ore Fluid Characteristics

Fluid inclusion (FI) analysis of samples from quartz vein host-rocks was conducted to gain insight into the nature of the hydrothermal fluids responsible for ore formation and to ascertain the pressure-temperature (P-T) conditions at which the minerals were deposited.

The samples were taken from specific depths in the GRD39-08_283.70m (FI 1), KL98-10-21_277.40m (FI1-4) at 304.30m (FI1-5), and KL98-10-22_706.80m (FI2-3), and 1398.30m (FI2-4). These samples were collected from both barren and weakly mineralized quartz veins within intensely phyllic-advanced argillic altered intrusive. The FI analysis aims to demonstrate the trapping of various fluid compositions during quartz precipitation.

At the prospect, three types of inclusions have been distinguished: Type I comprises H_2O- (CO_2)-NaCl or a combination of liquid, vapour, and halite; Type II involves H_2O-CO_2, both in liquid and vapour forms; and Type III is characterized by H_2O-CO_2-NaCl, encompassing liquid, vapour, halite, and some solid minerals, as indicated in Table 6.

The calculated salinities for both H_2O liquid and vapour phases, as well as NaCl content, indicate that the separated fluid phase from which this fluid originated was highly saline, containing upwards of >60 wt. % NaCl equivalent. Based on the Th and Tm diagram, which depicts a standard range for inclusions from diverse deposit types (Wilkinson, 2001), it was deduced that the Gajah Tidur area can be categorized as a porphyry-type deposit, with an overprint of epithermal advanced argillic alteration (Figure 16).

Fluid inclusion analysis has also indicated a moderate to high salinity, liquid-vapour-halite

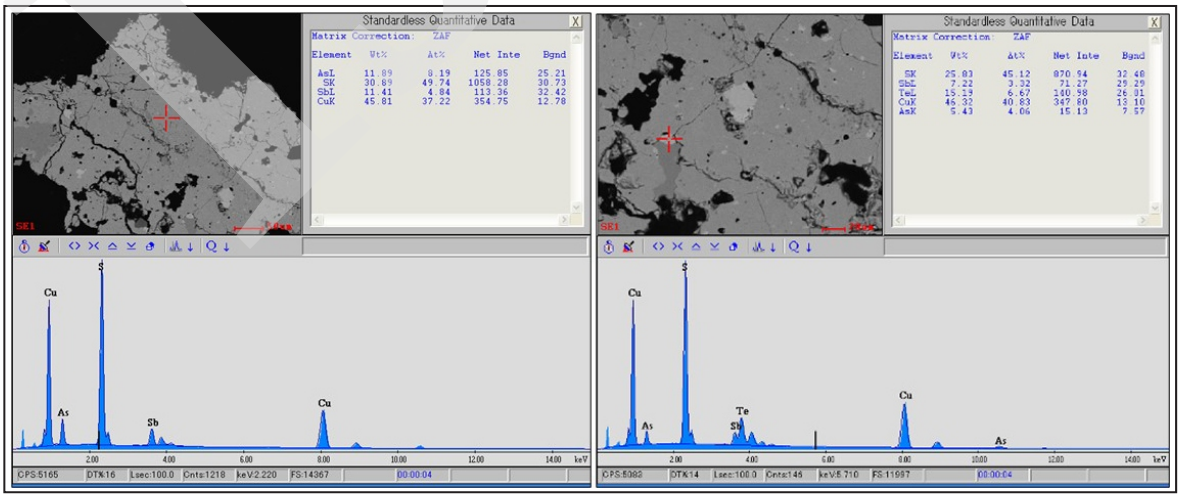

Figure 15. SEM-EDX result identifying Cu, As, and Sb elements from possible enargite with quartz veining in potassic altered Dalam diorite (GRD39-8 @114.10m depth) as a high sulphidation mineral assemblage.

Table 6. Fluid Inclusion Microthermometric Data Summary

Sample	n	Volume Fraction (vap)	Inclusion Type	Size (µm)	Bulk Density	Tm (CO_2)	Tm (ice)	(Tm (clath)	Th (total)	Salinity (eq% NaCl)
FI 1	32	0.15 - 0.47	I, II, III	4.04 - 18.42	0.12 - 1.11	-57.7 - (-54.7)	-9.8 - (-1.2)	2.3 - 15.7	160.3 - 241.3	30.15 - 34.05
FI 1-4	22	0.15 - 0.45	I, II, III	4.79 - 20.43	0.98 - 1.02	-59.4 - (-54.7)	-9.1 - (-0.4)	1.2 - 12.3	392.7 - 541.2	48.58 - 61.49
FI 1-5	16	0.15 - 0.49	I, II, III	7.62 - 34.16	0.61 - 0.88	-56.9 - (-53.9)	-5.1 - (-1.5)	5.4 - 7.8	403.7 - 540.2	52.25 - 65.35
FI 2-3	17	0.17 - 0.45	I, II, III	6.76 - 24.51	0.61 - 1.00	-58.8 - (-53.4)	-4.9 - (-0.5)	7.8 - 11.5	483.4 - 528.4	59.19 - 62.69
FI 2-4	24	0.15 - 0.45	I, II, III	4.69 - 17.43	0.70 - 1.06	-58.6 - (-50.9)	-8.7 - (-1.2)	1.3 - 13.2	483.7 - 542.3	59.32 - 63.23

Barren crystalline qyartz vein Qz-py-cp-bn vein Qz-py-cv vein

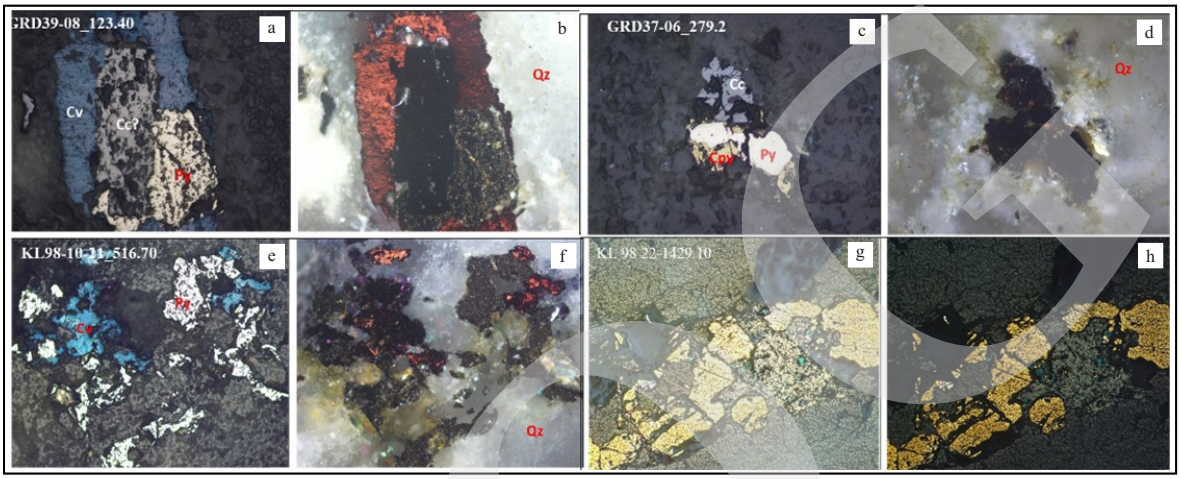

Figure 16. a). Cross polarized reflected light photomicrograph of covellite (cv)-pyrite (py)-chalcocite (cc), quartz stockwork vein (qv). Py (1st stage)-cc replaced by cv and intergrown with cc (2nd stage). b). Plane-polarized transmitted and reflected light photomicrograph from (a). c). x-polarized reflected light photomicrograph composed of py-cp and cc in qv. d). plane-polarized photomicrograph as in (c). e). x-polarized reflected light photomicrograph of composite py-cp and cv±enargite? intergrown and interstitial, in qv stockwork. f). Plane polarized photomicrograph of the same sample as e. g). x-polarized reflected light photomicrograph of cp-py replaced by bornite-cv interstitial and overgrown in qv stockwork. h). Plane-polarized reflected light similar to g, consisting of py-cp veins partially replaced by covellite.

and liquid-vapour types, which represent two separate phases of the hydrothermal system as the fluid pressure and temperature changes (Figure 17). This can cause the hydrothermal fluid system to move from one phase to the other. While liquid-vapour-halite with some solid minerals is possible to represent a supercritical fluid exsolved from a magma at depth. Fluid inclusion analysis has indicated two separate hydrothermal systems consisting of Gajah Tidur porphyry Cu-Mo and younger Main Grasberg porphyry Cu-Au.

Discussion

There are at least three alteration types and associated mineralization that have been identified at the studied area which hosted in GIC, Gajah Tidur Monzodiorite, and the wall rock. The alteration is related to typical porphyry style of alteration, consisting of potassic alteration as an early stage, dominated by pale brown biotite-K-feldspar and overprinted by phyllic-advanced argillic alteration. While advanced argillic and associated high sulphidation epithermal mineralization are less intense compared to more pervasive phyllic alteration, which overprints the stockwork and surrounding rocks, and emplaced at the upper part of the quartz stockwork and quartz flooding. It is possibly associated with the late stage Gajah Tidur Cu-Mo porphyry hydrothermal fluids becoming cooler and highly acidic.

Grasberg Igneous Complex (GIC) contains two porphyry systems (Leys *et al.*, 2020), which consist of Gajah Tidur Cu-Mo and Main Grasberg Cu-Au. Gajah Tidur porphyry monzonite (3.4 Ma)

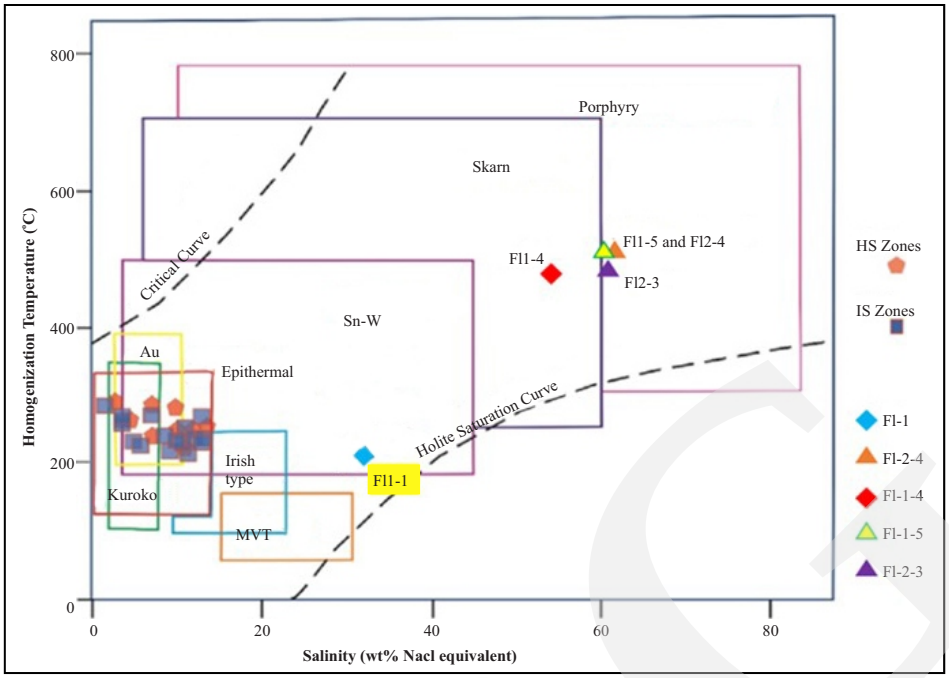

Figure 17. Fluid Inclusion salinity wt. % NaCl equivalent vs homogenization temperature (Th °C) of FI-1 that falls in Sn-W salinity and the other sample fall into Porphyry (see also Table 6).

has the peak at 2,750 m. It is overlain by quartz stockwork with a low-grade and strongly altered phyllic and quartz flooding, contained chalcopyrite-molybdenite veinlets. While Main Grasberg porphyry extends from the surface to 2,700 m elevation, strongly potassic altered monzodiorite, overprinted by quartz stockwork-magnetite veinlets, chalcopyrite, and less molybdenite. The altered and mineralized Main Grasberg and the surrounding Dalam rocks are then separated by the Kali dyke which is weakly mineralized to unmineralized.

Similar to the other porphyry system such as Oyu Tolgoi in Mongolia, the Gajah Tidur Cu-Mo porphyry did not have its hydrothermal fluids that rise to the surface to form lithocap. Instead, the ascending fluids cooled at shallower depths resulting in the formation of advanced argillic alteration. High sulphidation and associated argillic alteration at Gajah Tidur area are sporadic and occupy a smaller volume in comparison to more intensive phyllic alteration that covers a significant portion of both the stockwork and massive quartz alteration. This discrepancy might be attributed to the possibility that the last surge of Gajah Tidur hydrothermal fluids was limited in quantity and consequently cooled swiftly to temperatures of < 200 °C, as indicated by fluid inclusion homogenization temperatures (Th). This process led to an acidic environment, resulting in the replacement of sericite with advanced argillic minerals.

Pervasive phyllic and advanced argillic alteration emplaced beneath the higher level of Grasberg porphyry Cu-Au ore deposit are anomalous compared to other porphyry systems. Such extreme telescoping could be due to a high erosion rate, catastrophic unroofing, or reactivation of magmatic-hydrothermal activity after a prolonged hiatus with erosion and unroofing (Allen, 2015). Chalcopyrite at the base of the Grasberg ore zone and in the core of the Kucing Liar orebody is altered to ore-grade covellite. Covellite deeper in the system is minor, and there is no evidence in adjacent potassic-altered porphyry and syenite that copper grades were significant prior to phyllic and advanced argillic alteration, implying that copper was not very mobile in fluids causing phyllic and advanced argillic alteration.

Conclusions

Gajah Tidur is a separated Cu-Au-Mo porphyry that is older than the main Grasberg Cu-Au. Although it is separated and distinct porphyry system, there is some relationships with the Grasberg porphyry deposit. High sulphidation mineralization and associated argillic alteration overprinting phyllic alteration on the upper side of the quartz stockwork is probably originated from the late stage Gajah Tidur hydrothermal fluids which became cooler and highly acidic. Since Gajah Tidur is a deep porphyry system, its hydrothermal fluids did not reach the surface to form an epithermal lithocap, instead it ascended to the surface and cooled to form an advanced argillic alteration at depth.

Acknowledgments

This report stems from the primary author's post-graduate studies in economic geology at The Faculty of Geology, Universitas Padjadjaran, Bandung. Gratitude is extended to Mr. Aditya Pringgoprawiro, Managing Director of P.T. Eksplorasi Nusa Jaya, as well as Mr. George MacDonald, who initiated the exploration of Gajah Tidur and established the systematic XRD and multi-element geochemical analysis programme for the Ertsberg- Grasberg drill core samples. Thanks also go to Mr. Setyatmoko, Chief Geologist at P.T. ENJ, ENJ staff both on site and in Jakarta, Dr. Reza Al Furqan, Mr. Wahyu Sunyoto, former Senior VP Geology Engineering, and Mr. Ardhin Yuniar, VP Geology Engineering at P.T. F.I., along with Mr. Sugeng Widodo, Exploration Manager at Freeport McMoRan Inc. for granting permission to utilize and to gather data for the publication of this paper. The first author personally funded the research.

References

Al Furqan, R., 2020. *Hydrothermal Alteration and Fluid Evolution of The Deep Grasberg Porphyry System, Papua, Indonesia*, Final Desertation, Department of Earth Resource Science, Akita University.

Allen, J.M., 2012. Deep Grasberg Exploration:The KL98 Drill section and Evolution of the GIC. John Allen & Associates Ltd, Geology. Petrology Consultant.

Cloos, M., Sapiie, B., Ufford, Quarles van, Weiland, R.J., Warren, P.Q., and McMahon, T.P., 2005. Collisional delamination in New Guinea: The geotectonics of subducting slab breakoff. *Geological Society of America Special Paper* 400, 51pp.

Cox, K.G., Bell, J.D., and Pankhurst, R.J., 1979. Compositional variation in magmas. *In*: *The Interpretation of Igneous Rocks*. Springer, Dordrecht, Netherlands, 455p. DOI: 10.1007/978-94-017-3373-1_2

Dewey, J.F. and Bird, J.M., 1970. Mountain belts and the new global tectonics. *Journal of Geophysical Research,* 75*,* p.2625-2647.

Hedenquist, J.W. dan Arribas, A., 2022. Exploration Implications of Multiple Formation Environments of Advanced Argillic Minerals. *Economic Geology,* 117 (3), p.609-643.

Leys, Clyde A., Schwarz, A., Cloos, M., Widodo, S., Kyle, J.R., and Sirait, J., 2020. *Grasberg Copper-Gold-R*. P.T. Freeport Indonesia.

MacDonald, G.D. and Arnold, L.C., 1994. Geological and geochemical zoning of The Grasberg Igneous Complex, Irian Jaya, Indonesia. *Journal of Geochemical Exploration,* 50*,* p.143-178.

McMahon, T.P., 1994a. Pliocene intrusions in The Gunung Bijih (Ertsberg) mining district, Irian Jaya, Indonesia; Major and trace element chemistry. *International Geology Review,* 36*,* p.925-946.

Mernagh, T.P., Leys, C., and Henley, R., 2020. *Fluid inclusion systematics in porphyry copper deposits: The super-giant Grasberg deposit, Indonesia as a case study*, Research School of Earth Sciences, The Australian National University, ACT2601.

Mernagh T.P. and Mavrogenes, J., 2019. Significance of high temperature fluids and melts in

The Grasberg porphyry copper-gold deposit, *Chemical Geology,* 508, p.210-224.

Sapiie, B., 1998. *Strike-slip faulting, breccia formation and porphyry Cu-Au mineralization in The Gunung Bijih (Ertsberg) mining district, Irian Jaya, Indonesia*. Unpub. Ph.D thesis, University of Texas Austin, 304pp.

Paterson, J.T. and Cloos, M., 2005. *Grasberg Porphyry Cu-Au Deposit, Papua, Indonesia: Magmatic History. In*: Porter, T.M. (ed.), *Super Porphyry Copper and Gold Deposits*: A Global Perspective, PGC Publishing, Adelaide, p.321-345

Sapiie, B. and Cloos, M., 2004. Strike-slip faulting in the core of The Central Range of West New Guinea: Ertsberg Mining District, Indonesia. *Geological Society of American Bulletin,* 116, p.227-293.

Trautman, M.C., 2013. *Hidden Intrusions and Molybdenite Mineralization beneath The Kucing Liar Skarn, Ertsberg-Grasberg Mining District, Papua, Indonesia.* Thesis Presented to the Faculty of the Graduate School of The University of Texas at Austin in Partial Fulfillment of the Requirements for the Degree of Master of Science in Geological Sciences The University of Texas at Austin August, 2013.

Ufford, Quarles van, 1996. *Stratigraphy, structural geology, and tectonics of a young forearc-continent collision, western Central Range, Irian Jaya (western Papua).* Unpub. Ph.D. thesis, University of Texas Austin, 421pp.

Wafforn, S.,Seman, S., Kyle, J.R., Stockli, D.F., 2018. Andradite garnet U-Pb geochronology of the big Gossan skarn, Ertsberg-Grasberg mining district, Indonesia. *Economic Geology,* 113 (3), p.769-778. DOI:10.5382/econgeo.2018.4569

Weiland, R.J. and Cloos, M., 1996, Pliocene-Pleistocene asymmetric unroofing of The Irian fold belt, Irian Jaya, Indonesia: Apatite fission-track thermochronology. *Geological Society of America Bulletin,* 108, p.1438-1449.